Proceedings of the Eighteenth International Conference on
Civil, Structural and Environmental Engineering Computing
Edited by: P. Iványi, J. Kruis and B.H.V. Topping
Civil-Comp Conferences, Volume 10, Paper 13.1
Civil-Comp Press, Edinburgh, United Kingdom, 2025
ISSN: 2753-3239, doi: 10.4203/ccc.10.13.1

Influence of Material and Shape Imperfections on Buckling of Externally Pressurized Auxetic Domes

J. Blachut and M. D. White

**Department of Mechanical and Aerospace Engineering,
University of Liverpool,
United Kingdom**

Abstract

This study offers a very first inside into the influence of imperfections on buckling of: (i) single-layer auxetic, and (ii) two-layer (steel–auxetic), shell subjected to external pressure. For the first case: modulated eigen-affine imperfections show little difference between Poisson's ratio of 0.3, and negative Poisson's ratio of -0.5. The same proved to be true for a localised inward, Force-Induced-Dimple, (FID). Significant variations in the localised wall thickness of auxetic layer resulted only in minute drop of buckling pressure. The same became true for localised, large perturbation in the magnitude of negative Poisson's ratio.
For the case two, the wall thickness was made half steel and halve auxetic. The shell with Poisson's 0.3 and -0.5, shows markedly larger sensitivity when compared with results obtained for Poisson's equal to 0.3 in both layers, i.e., on a like-for-like basis this shell is less safe. This is true for both eigen-affine imperfections as well as for Force-Induced-Dimple.

Keywords: mechanical metamaterials, auxetics, negative Poisson's ratio, elastic-plastic, external pressure, buckling, imperfections.

1 Introduction

This study refers to a subset of metamaterials known as auxetics. Auxetic materials can be broadly divided into natural auxetics and man-made. Intensive studies into engineered, man-made auxetics appear to have started about three decades ago. Auxetics expand in the lateral direction when stretched longitudinally, i.e., they bulge

when pulled. Also, under axial compression they become thinner in the lateral direction. Such behavior leads to a Negative Poisson's Ratio, NPR. Materials and structures that demonstrate auxetic behaviour, and whose base material are metal - are defined as metallic auxetics and auxetic structures.

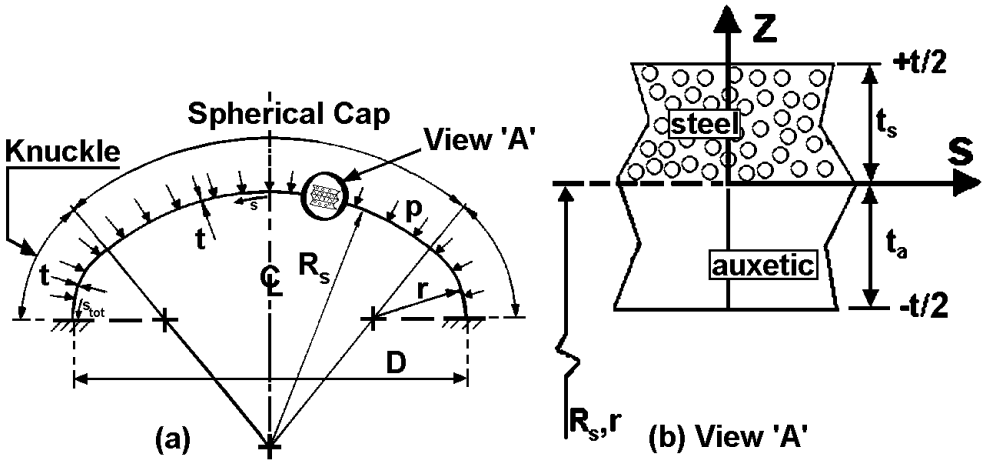

Figure 1: Geometry of torispherical shell (Fig. 1a), and two-layer wall thickness (Fig. 1b).

Properties of these novel materials open the possibility of wide practical applications across countless multiphysics fields, e.g., electromagnetics, acoustic stealth, optical communications, thermal camouflage, References [1-3]. These futuristic auxetics continue to attract a lot of research in structural mechanics, References [4-9]. Typical structural elements (plates, cylinders, cones), are considered here in various wall configurations. Auxetic metals with the Poisson's ratio approaching, $\upsilon = -1.0$, have been reported, Reference [4]. Also, auxetics having isotropic properties are reported in Reference [10]. Metallic auxetics show a similar stress-strain profile as in their base material. For example, auxetics derived from the base material being stainless steel show a similar stress-strain relationship (but only with nominal strain for up to 0.16), Reference [4].

Auxetics are also actively examined in the area of composites, where the following research categories can be identified: (a) one-dimensional (auxetic fibres, yarns), (b) two-dimensional (auxetic ply, textiles), and (c) three-dimensional auxetic (composites), References [11-12].

Anticipating arrival of auxetics to manufacturing of doubly curved shells – this study assesses how various imperfections would affect the buckling behaviour of these shells when subjected to quasi-static, uniform external pressure. A typical end-closure onto cylindrical pressure vessel is taken as an example, i.e., shell of torispherical geometry. This is entirely numerical study based on the existing FE-technology.

2 Single-layer auxetic torisphere

2.1 Perfect torisphere

Consider torispherical shell with its geometry parameters shown in Figure 1a. Assume $R_s/D = 1.0$, the knuckle-radius-to-diameter ratio (r/D) = 0.1, and the (D/t)-ratio, D/t =

1000. Let the shell be fully clamped at the equatorial plane, and subjected to quasi-static external pressure, p. Its material properties being given by the Young's modulus E = 210.0 GPa, and the yield point of material, σ_{yp}, equal to 350.0 MPa. The material of analysed shells is assumed to be isotropic.

	Bosor5		Abaqus		
ν	Indic(-2)	Indic(0)	(SAX2-Riks)	(S8R)	(S8R-Riks)
+0.30	0.122(17)	0.136(coll)	0.135(coll)	0.122(17)	0.135(coll)
-0.50	0.122(15)	0.128(coll)	0.128(coll)	0.123(16)	0.128(coll)
-0.75	---	0.132(coll)	0.131(coll)	---	0.131(coll)
-0.90	---	0.133(col)	0.133(coll)	---	0.133(coll)

Table 1: Comparison of failure pressures (bifurcation or collapse) for a single layer torisphere. Note: numbers in brackets refer to number of circumferential waves at bifurcation; coll ≡ axisymmetric collapse; D/t = 1000, R_s/D = 1.0, r/D = 0.10, E = 210 GPa, σ_{yp} = 350MPa;

Under external pressure the above dome can fail either through asymmetric bifurcation buckling with a number of circumferential waves or by axisymmetric collapse. The following two software codes, capable of estimating magnitudes of both failure mechanisms, are used, i.e., Abaqus – Reference [13] and Bosor5 – Reference [14]. Linear elastic, perfectly plastic modelling of the shell's material is adopted in both types of analyses. The range of the Negative Poisson's Ratio, NPR, investigated varies between υ = +0.3 and υ = -0.9. Table 1 provides the results for the NPRs = +0.30, -0.50, -0.75, and -0.90.

In the FE code Abaqus, prediction of the bifurcation mode is based on the use of 8-node shell element S8R. Convergence of results was secured here for 160 elements along the meridian and 240 elements along the circumference. Collapse mode was

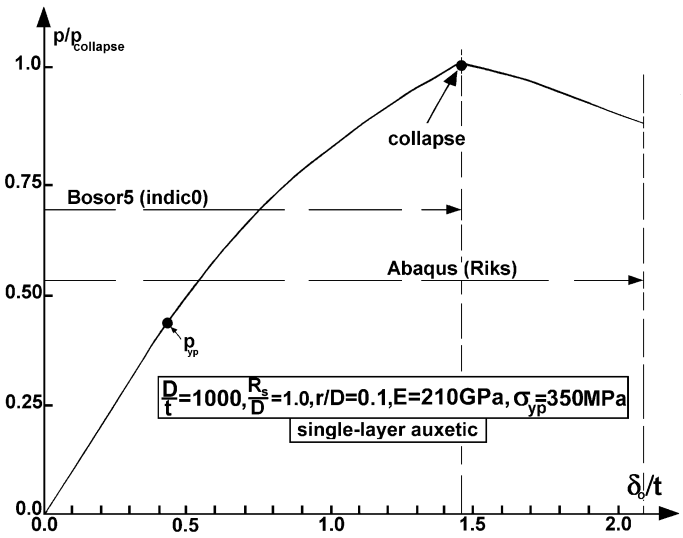

Figure 2: Load-apex deflection curve as obtained from Abaqus and Bosor5 codes. Note: p_{yp} ≡ first yield pressure.

computed using shell elements, S8R, as well as axisymmetric shell element, SAX2. Eighty equally spaced SAX2 along the meridian secured the convergence. Bosor5 required 140 mesh points along the meridian to obtain converged solutions. Predictions of magnitudes of various failure modes given by both codes are the same, as seen in Table 1. Also, the eigenmode given by both codes is the same, i.e., n = 17 waves in hoop direction for the case of $\nu = +0.3$. For the case of $\nu = -0.5$ they are 15 and 16, respectfully. Magnitudes of axisymmetric collapse pressure are identical for axisymmetric analyses (SAX2), and for 2D analyses using shell elements S8R. Estimates of collapse loads using Bsosor5 Indic0-option are nearly the same as those given by Abaqus code. It is worth noting here that the estimation of bifurcation buckling by Abaqus is not universally valid/recommended – as mentioned in the code's manuals. Also, the load versus apex deflection curves are the same for up to the collapse level as seen in Figure 2. The Riks option in the FE code Abaqus allows to trace the apex deflection beyond the collapse. But from practical point this is irrelevant since there is no residual strength beyond the collapse pressure, and the shell is destroyed as seen in published results of experiments.

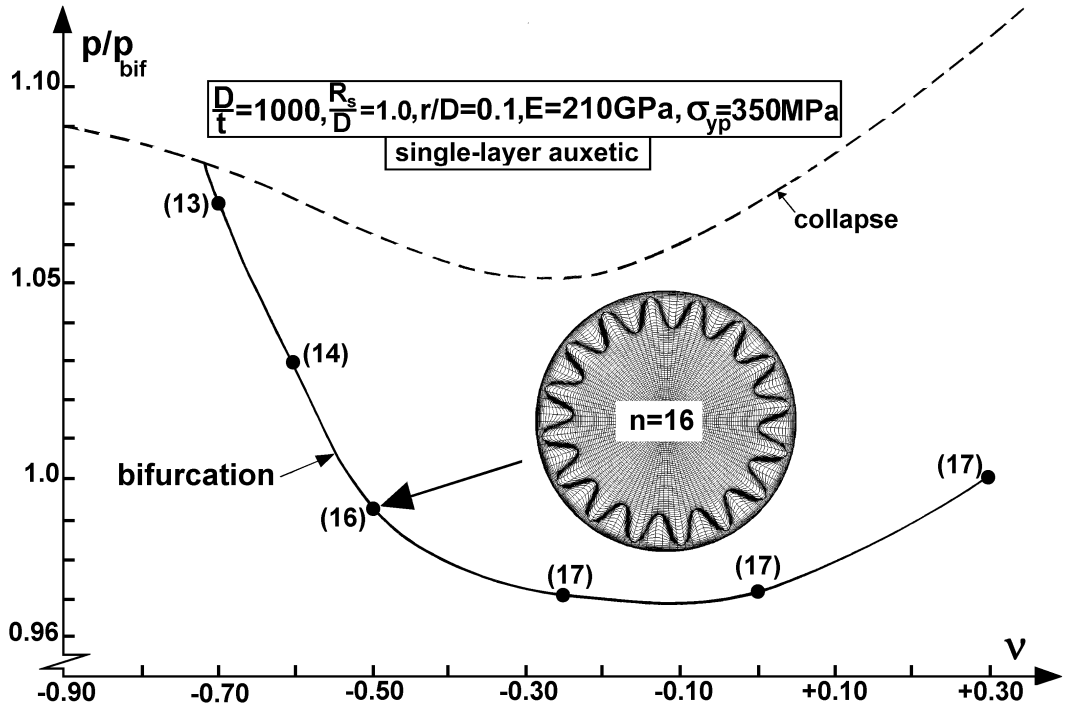

Figure 3: Plot of bifurcation buckling and collapse pressure versus Poisson's ratio, υ. Note: No. of hoop waves at bifurcation shown in brackets.

Figure 3 plots values of asymmetric bifurcation buckling and axisymmetric collapse for Poisson's ratio between $\upsilon = +0.30$ and $\upsilon = -0.90$. It is seen here that bifurcation buckling remains the controlling mechanism of failure between $\upsilon = +0.30$ an $\upsilon \approx -0.72$. Axisymmetric mode of failure is active for: $-0.90 \leq \upsilon < 0.72$. The insert in Figure 3 depicts eigenmode for $\upsilon = -0.50$ with n = 16 circumferential number of waves (as seen from above).

2.2 Imperfect torisphere

Unavoidable imperfections in shape of externally pressurised domes (hemispheres, spherical caps, torispheres, ellipsoids, etc.), can severely affect the magnitude and mechanism of failure of these shells, e.g., References [15-18]. Over the last several decades a lot of know-how has been accumulated regarding this topic. This has led to the establishment of design codes, e.g., References [19-22]. Arrival of auxetic shells brings new issues in imperfection sensitivity of buckling pressure. Apart from initial shape deviation from perfect geometry, the influence of imperfect wall thickness, associated variability of NPR, have to be assessed in order to quantify how they influence the buckling strength.
In what follows, some answers to the above issues are examined through selective parametric studies.

δ/t	υ = +0.30	υ = -0.50
	p/p_{bif}	
0.25	0.66	0.69
0.5	0.44	0.51
1.0	0.35	0.31
1.5	0.30	0.31
2.0	0.28	0.30

Table 2: Comparison of sensitivity of buckling pressure to Force-Induced-Dimple imperfection for υ = +0.30 and υ = -0.50 in a single layer auxetic torisphere. Note: $\frac{\delta}{t} \equiv$ magnitude of inward dimple.

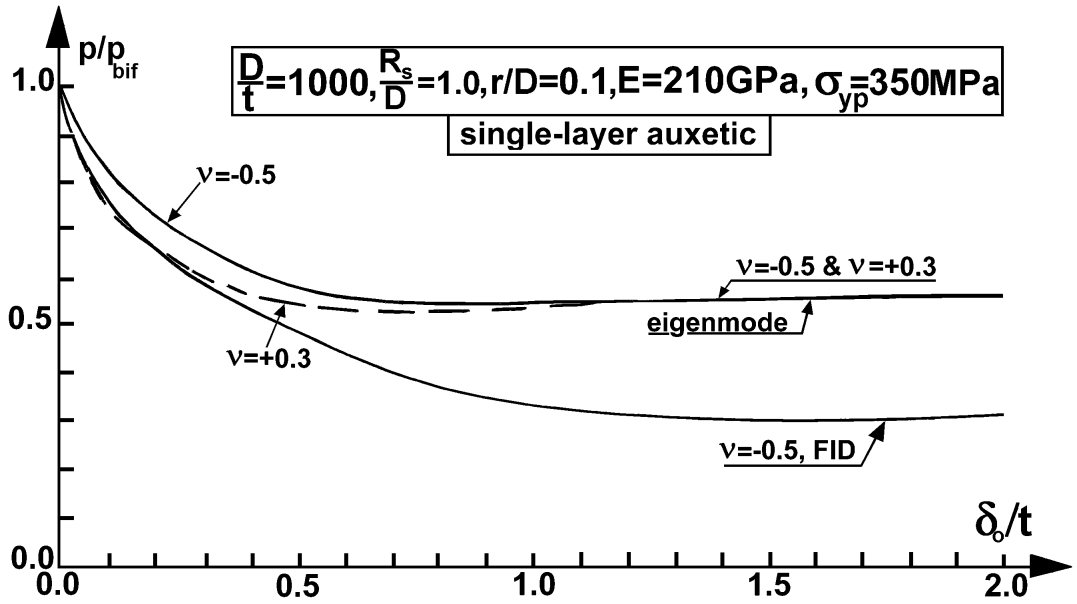

Figure 4: Imperfection sensitivity of buckling pressure for a single layer auxetic torisphere. Note: FID ≡ Force Induced Dimple imperfection at s/s_{tot} = 0.70;

2.2.1 Initial shape imperfections

Several different approaches have been used in the past, to estimate the sensitivity of buckling pressure to initial geometric imperfections, e.g., eigenmode affine, increased-radius lower bound, and local inward dimple, Reference [16]. Figure 4 depicts results for some initial shape imperfections being studied in the past. It has been, for example, customary to adopt the initial shape deviations in the form of modulated eigenmode. The eigenshape with n = 17, was taken as a possible imperfection for the case $\upsilon = +0.30$. The eigenmode with n = 16 was taken for $\upsilon = -0.50$. The amplitude of imperfection, δ/t, was varied between $\delta/t = 0$ and $\delta/t = 2.0$. Results seen in Figure 4 indicate that 'the sensitivity profile' remains comparable for both $\upsilon = +0.30$ and $\upsilon = -0.59$. Only for small values of the (δ/t)-ratio the NPR case offers smaller reduction of buckling pressure. Another form of analysed geometrical deviation from perfect geometry was a localised inward dimple created by a concentrated force – known in the literature as Force-Induced-Dimple, FID. For this case a much worse reduction of buckling pressure was recorded than for the modulated eigenshape. Figure 4 depicts results for, $\upsilon = -0.50$, and Table 2 gives selected results for $\upsilon = +0.30$. It is seen here that there is no great difference between both cases.

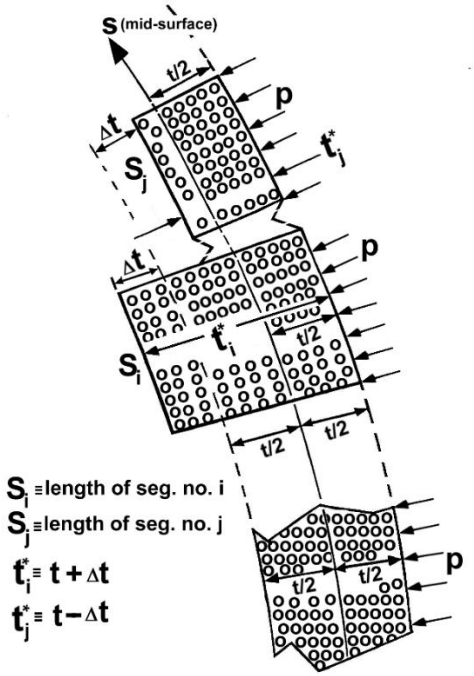

Figure 5: Illustration of variable wall thickness on inner side.

2.2.2 Imperfect wall thickness and variable NPR

Assume that the wall thickness of the inner side of the auxetic layer is imperfect since the outer side is, eventually, to be attached to the 'nearly perfect metallic layer'. Assume that there are N-segments of piece-wise constant wall thicknesses as illustrated in Figure 5, and each of meridional length is, $s_i = s_{tot}/N$, where $s_{tot}/D =$

0.572. The magnitude of wall thickness within each segment is allowed to be varied by, $\Delta t_i = \pm t/2$. Comparison is provided between the NPR-auxetic layer, $\upsilon = -0{,}50$, with a steel layer with Poisson's ratio, $\upsilon = +0.30$. Detailed results for N = 2 are given in Table 3. It is seen that the largest dimensionless buckling pressure drop is to 0.55 for $\upsilon = +0.30$, and to 0.60 for $\upsilon = -0.50$. Hence for this case the auxetic shell can support larger pressure, i.e., the buckling pressure is less sensitive to a similar change in wall thickness.

υ	p/p_{bif}								
	configuration								
	1-2	2-1	1-0	0-1	2-0	0-2	0-0	1-1	2-2
-0.50	0.60(18)	1.07(13)	1.0(15)	1.47(13)	1.0(15)	0.60(18)	1.0(15)	1.47(13)	0.60(18)
+0.30	0.55(20)	1.0(13)	0.98(17)	1.48(14)	0.98(17)	0.56(20)	1.0(16)	1.48(14)	0.55(20)

Table 3: Buckling pressure for piece-wise wall thicknesses – comparison of results between NPR, $\upsilon = -0.50$, and Poisson's, $\upsilon = +0.30$. Note: The first digit in configuration denotes segment one (starting from apex); The second one denotes segment no. 2 (ending at clamped edge). Also: '1' ≡ 1.25t, '2' ≡ 0.75t, '0' ≡ t.

Another imperfection might be associated with non-perfect distribution of magnitude of NPR. Hence two types of structural response to variation of NPR were also carried out. In the first one two different values of NPR were assigned to spherical cap and knuckle, i.e., $\upsilon = -0.90$ ($s/s_{tot} \equiv [0.0, 0.81]$) for spherical cap, and $\upsilon = -0.45$ ($s/s_{tot} \equiv (0.81, 1.0]$) for the knuckle. The computed ratio of (p/p_{coll}), was 1.0. This means that the reduced value (50%), of NPR over sizeable length of the meridian did not reduce the magnitude of collapse pressure. At the next stage the values of NPRs were switched between segments, i.e., $\upsilon = -0.45$ ($s/s_{tot} \equiv [0.0, 0.81]$), and $\upsilon = -0.90$ ($s/s_{tot} \equiv (0.81, 1.0]$, knuckle). In this case, the computed ratio of (p/p_{coll}), was 0.97. Again, the computed drop of the collapse pressure is very small.

s/s_{tot}	[0.0-0.1]	[0.1-0.2	[0.2-0.3]	[0.3-0.4]	[0.4-0.5]	[0.5-0.6]	[0.6-0.7]	[0.7-0.8]	[0.8-0.9]	[0.9-1.0]
υ	-0.45	-0.45	-0.45	-0.45	-0.45	-0.45	-0.45	-0.45	-0.45	-0.45
p/p_{coll}	1.0	1.0	1.0	1.0	1.01	1.01	1.01	0.98	1.0	1.0

Table 4: Collapse pressures for localised NPR, $\upsilon = -0.45$, in ten segments of 10% meridional arc length, s/s_{tot}. Note: '0.0' in segment, [0.0-0.10], denotes apex. The last column on the right corresponds to the segment adjacent to the clamped edge.

The full length of the meridian was divided into ten segments of equal length as another way of assessing sensitivity of collapse pressure. The values of NPR, $\upsilon = -0.45$, were assigned to each segment in turn while the remaining parts of the meridian had, $\upsilon = -0.90$. Results for all ten segments are given in Table 4. It is seen here that over large portion of the meridian there is no reduction in magnitude of collapse pressure. The only reduction was recorded for the segment spanning, $s/s_{tot} = [0.7\text{-}0.8]$ with recorded drop to 0.98. Again, this is a very small reduction in collapse pressure for a 50% change in NPR's magnitude.

3 Two-layer auxetic torisphere

One of possible application of metamaterials analysed here is a two-layer shell subjected to eternal pressure. As the auxetic material is to be porous, the practical arrangement would require the external layer to be from conventional steel supported on inside by an auxetic layer (as illustrated in Figure 1b). Consider the previous torisphere's configuration with the only one exception regarding the composition of the wall thickness. Divide the full thickness, t, into the outer layer having the thickness, t/2, and the inner auxetic layer having the same thickness, i.e., t/2. Two types of initial shape imperfections were adopted in order to check the response of buckling pressure. They were: eigenmode affine shape deviation from perfect geometry, and inward, localised dimple positioned at $s/s_{tot} = 0.70$. Results are shown in Figure 6, where comparison is given with the response to steel only shell (i.e., with $\upsilon = +0.3$). It is seen here that the auxetic shell reduced the buckling load by larger amount than the corresponding shell with, $\upsilon = +0.30$.

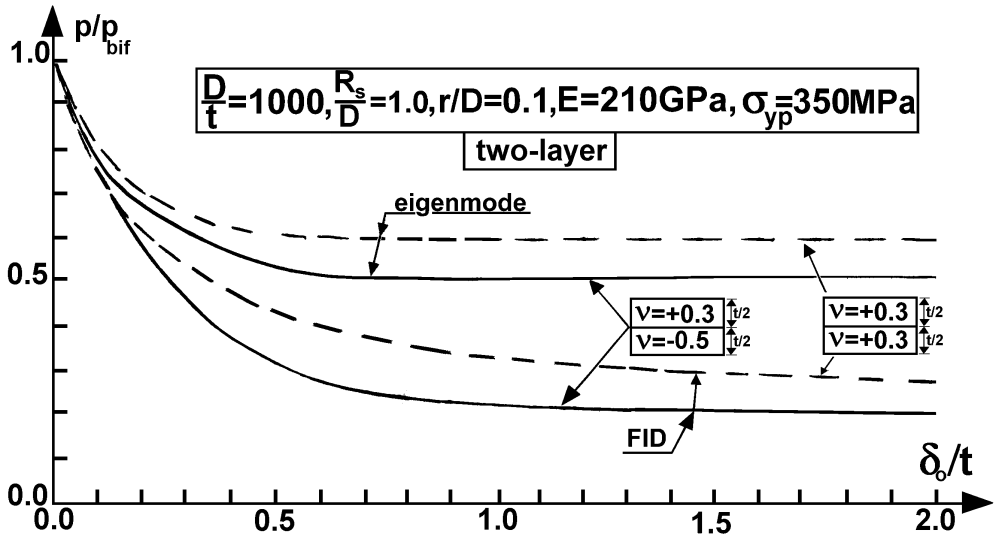

Figure 6: Imperfection sensitivity of buckling pressure for a two-layer auxetic torisphere. Note: FID ≡ Force Induced Dimple imperfection at $s/s_{tot} = 0.70$;

4 Conclusions

This study reveals different sensitivity of buckling pressure to imperfections for a single layer, auxetic shell, and different for a two-layer wall.

The initial shape imperfections in a single, auxetic wall follow a similar 'sensitivity trend' as in a dome made from steel, only. Also, magnitudes of pressure drop remain nearly the same. Some large perturbations in the wall thickness and in values of NPRs resulted only in minute reduction of buckling pressure. This is a significant observation as it would help manufacturing of auxetic layers aimed at doubly curved shells. Hence wider studies of this would be highly desired.

Initial shape imperfections in a two-layer wall [50%-steel, 50%-auxetic], substantially reduce the buckling pressure for both eigen-affine and for inward Force-Induced-

Dimple profiles when compared with [50%-steel, 50%-steel], i.e., for a like-for-like configuration. Again, a definitive conclusion will require a wider/comprehensive study.

References

[1] Y. Zheng, H. Dai, J. Wu, Ch. Zhou, Z. Wang, R. Zhou, W. Li, "Research progress and development trend of smart metamaterials", Frontiers in Physics, vol. 10, 2022, 1069722, 1-11.

[2] M. Askari, D.A. Hutchins, P.J. Thomas, L. Astolfi, R.L. Watson, M. Abdi, M. Ricci, S. Laureti, L. Nie, S. Freear, R. Wildman, Ch. Tuck, M. Clarke, E. Woods, A.T. Clare, "Additive manufacturing of metamaterials: a review", Additive Manufacturing, vol. 36, 2020, 101562, 1-36.

[3] L. Zhou, X. Zheng, K. Du, X. Guo, Q. Yin, A. Lu, Y. Yi, "Parametric and experiment studies of 3D auxetic lattices based on hollow shell cuboctahedron", Smart Materials and Structures, vol. 30, 2021, 025042, 1-10.

[4] D. Han, X. Ren, Y. Zhang, X.Y. Zhang, X.G. Zhang, Ch. Luo, Y.M, Xie, "Lightweight auxetic metamaterials: design and characteristic study", Composite Structures, vol. 293, 2022, 115706, 1-11.

[5] M.I. Khan, M. Umair, Y. Nawab, "Use of auxetic material for impact/ballistic applications", pp 199-228, in '*Composite Solutions for Ballistics'*, (eds) Y. Nawab, S.M. Sapuan, K. Shaker, Woodhead Publishing, Duxford CB22 4QH, U.K., 2021, pp 1-300.

[6] Y. Zhou, D. Jiang, L. Wang, P. Xiang, L-J. Jia, "Cushioning performance of origami negative Poisson's ratio honeycomb steel structure", Thin-Walled Structures, vol. 204, 2024, 112284, 1-13.

[7] Ch. Mercer, T. Speck, J. Lee, D.S. Balint, M. Thielen, "Effects of geometry and boundary constraint on the stiffness and negative Poisson's ratio behaviour of auxetic metamaterials under quasi-static and impact loading", International Journal of Impact Engineering, vol. 169, 2022, 104315, 1-12.

[8] P.T. Thang, Ch. Kim, H. Jang, T. Kim, J. Kim, "Buckling behaviour analysis of hybrid-honeycomb sandwich cylindrical shells", Ocean Engineering, vol. 276, 2023, 114214, 1–12.

[9] V. Siniauskaya, H. Wang, Y. Liu, Y. Chen, M. Zhuravkov, Y. Lyu, "A review on the auxetic mechanical metamaterials and their applications in the field of applied engineering", Frontiers in Materials, vol. 11(August), 2024, 1-14, (doi: 10.3389/fmats.2024.1453905).

[10] J.N. Grima, R. Gatt, A. Alderson, K.E. Evans, "On the auxetic properties of 'Rotating Rectangles' with different connectivity", Journal of the Physical Society of Japan, vol. 74(10), 2005, 2866-2867.

[11] H. Iftekhar, R.M.W.U. Khan, Y. Nawab, S.T.A. Hamdani, S. Panchal, "Numerical analysis of binding yarn float length for 3D auxetic structures", Physica Status Solidi B – Basic Solid State Physics, vol. 257(10), 2020, 1-8.

[12] S. Shukla, B.K. Behera, "Auxetic fibrous structures and their composites: a review", Composite Structures, vol. 290, 2022, 115530, 1-28.

[13] Hibbitt, Karlsson, Sorensen Inc. 2006. ABAQUS – Theory and Standard User's Manual Version 6.4, Pawtucket, RI, 02860-4847, USA.
[14] D. Bushnell, "Bosor5: program for buckling of elastic-plastic complex shells of revolution including large deflections and creep", Computers and Structures, vol. 6, 1976, 221-239.
[15] C.R. Calladine, "Understanding imperfection-sensitivity in the buckling of thin-walled shells", Thin- Walled Structures, vol. 23, 1995, 215-235.
[16] J. Błachut, O.R. Jaiswal, "On the choice of initial geometric imperfections in externally pressurized shells", Journal of Pressure Vessel Technology, Transactions of the ASME, vol. 121, 1999, 71-76.
[17] W. Wunderlich, U. Albertine, "Buckling behaviour of imperfect spherical shells", International Journal of Non-linear Mechanics, vol. 37, 2002, 589-604.
[18] J.M. Rotter, "The new framework for shell buckling design and European shell buckling recommendations", Journal of Pressure Vessel Technology, Transactions of the ASME, vol. 133, 2011, 011202.
[19] NASA, Buckling of Thin-Walled Doubly Curved Shells, NASA, Space Vehicle Design Criteria (Structures), Report No. NASA SP-8032, 1969, 1–33.
[20] ASME, "Alternative Rules for Determining Allowable External Pressure and Compressive Stresses for Cylinders, Cones, Sphere and Formed Heads, Section VIII, Divisions 1 and 2", Cases of the ASME Boiler and Pressure Vessel Code, American Society of Mechanical Engineers, New York, Standard Code Case 2286-2, 2008, 1-13.
[21] ECCS, "Buckling of Steel Shells – European Design Recommendations", ECCS TC8 TWG 8.4 Shells, vol. 125, 5th Edition, Multicomp Lda, Algueirao-Mem Martins, Portugal, 2008, 384p.
[22] PD 5500, Public Document, British Standards Institution, London, 9th Edition, 2024.